Next-to-next-to-leading-order ϵ expansion for a Fermi gas at infinite scattering length

Peter Arnold
Department of Physics, University of Virginia, Box 400714, Charlottesville, Virginia 22904-4714, USA

Joaquín E. Drut and Dam Thanh Son
Institute for Nuclear Theory, University of Washington, Seattle, Washington 98195-1550, USA

(Received 23 August 2006; revised manuscript received 29 January 2007; published 5 April 2007)

We extend previous work on applying the ϵ expansion to universal properties of a cold, dilute Fermi gas in the unitary regime of infinite scattering length. We compute the ratio $\xi=\mu/\epsilon_F$ of chemical potential to ideal gas Fermi energy to next-to-next-to-leading-order (NNLO) in $\epsilon=4-d$, where d is the number of spatial dimensions. We also explore the nature of corrections from the order after NNLO.

DOI: 10.1103/PhysRevA.75.043605 PACS number(s): 03.75.Hh, 05.30.Fk, 21.65.+f

I. INTRODUCTION AND RESULTS

For a number of years, it has been a challenge to compute the properties of a dilute Fermi gas with infinite scattering length [1]. This is known as the unitary regime and is relevant to cold systems for which the interparticle separation is very small compared to the two-particle scattering length a, but very large compared to any other distance scales r characterizing two-body interactions: $a \gg n^{-1/3} \gg r$, where n is the density. In the unitary regime, the only dimensionful parameter is the number density n, and so all physical quantities in this limit should be determined by dimensional analysis and universal constants of proportionality. Dimensionless ratios will be universal [2]. There has been much interest in recent years in attempting to compute such universal constants of the unitary regime (see, e.g., Refs. [3,4] and references therein).

The problem is nonperturbative in three spatial dimensions. However, inspired by earlier work of Nussinov and Nussinov [5] on the behavior of the unitary regime as a function of spatial dimension d, it was recently realized [6] that, with an appropriately formulated perturbation theory, a perturbative solution is possible in $d=4-\epsilon$ spatial dimensions when $\epsilon \ll 1$. Results can be expressed as an asymptotic series in ϵ, analogous to the ϵ expansion methods that have been used with great success for 30 years to determine critical exponents in a variety of second-order phase transitions. One may then extrapolate to the case of three dimensions, $\epsilon=1$. For the case of cold, dilute Fermi gases at infinite scattering length, it is found [6] that

$$\xi \equiv \frac{\mu}{\epsilon_F} = \tfrac{1}{2}\epsilon^{\epsilon/2d}[\epsilon^{3/2} - 0.0492\epsilon^{5/2} + O(\epsilon^{7/2})]$$
$$= \tfrac{1}{2}\epsilon^{3/2} + \tfrac{1}{16}\epsilon^{5/2}\ln\epsilon - 0.0246\epsilon^{5/2} + \cdots, \quad (1.1)$$

$$\frac{\epsilon_0}{\mu} = 2 + O(\epsilon), \quad (1.2)$$

$$\frac{\Delta}{\mu} = \frac{2}{\epsilon} - 0.691 + O(\epsilon), \quad (1.3)$$

where μ is the chemical potential, Δ is the gap for fermionic excitations, and ϵ_0 is the value of $p^2/2m$ for fermionic excitations with the minimum energy Δ. The Fermi energy ϵ_F is defined as the Fermi energy of an ideal Fermi gas with the same density n as the strongly interacting gas under consideration.

The ratio ξ can be equivalently expressed as an energy density ratio[1]

$$\xi = \frac{\mathcal{E}}{\mathcal{E}_0}, \quad (1.4)$$

where $\mathcal{E}$ and $\mathcal{E}_0$ are the energy densities in the interacting and noninteracting cases, respectively, at equal number density n. For experimental relevance, ξ can also be expressed as [7,8]

$$\xi = \left(\frac{E^{\rm rel}}{E_0^{\rm rel}}\right)^2 \quad \text{(harmonic trap)} \quad (1.5)$$

for a system in a harmonic trap (in the limit of an arbitrarily wide trap), where the "release" energies $E^{\rm rel}$ and $E_0^{\rm rel}$ are the total system energies in the interacting and noninteracting cases at equal total particle number N.

Historically, in the simplest application of the ϵ expansion, one computes the first two or three terms in the ϵ expansion and sees if they are reasonably well behaved for $\epsilon=1$, which corresponds to three spatial dimensions. Using this method, the above expansions would give the estimates [6]

$$\xi \simeq 0.475, \quad \frac{\epsilon_0}{\mu} \simeq 2, \quad \frac{\Delta}{\mu} \simeq 1.31. \quad (1.6)$$

In this method, it is important to quit when one is ahead: Because the ϵ expansion is asymptotic, higher-order terms eventually grow. The simple procedure is to stop including higher-order terms when this happens. In more sophisticated applications of the ϵ expansion, however, critical exponents have been determined fairly precisely for some phase transitions by combining high-order ϵ expansions, information about the large-order asymptotic behavior, and knowledge of the behavior at or near lower dimensions such as $d=2$, to fit results as a function of dimension using Borel-Padé approxi-

[1] This can be proven simply by using thermodynamics and scaling at unitarity [2].

mations [9–12].[2] A similar procedure has recently been carried out for the ratio $\xi=\mu/\epsilon_F$ in Ref. [13] using next-to-leading-order results for the ϵ expansion about both four and two spatial dimensions (except that the high-order asymptotic behavior of the ϵ expansion about four dimensions is currently unknown).

The goal of the current paper is to take the step of computing the next term in the ϵ expansion about four spatial dimensions for ξ at zero temperature, and to learn something about the analytic structure in ϵ by showing that new, nontrivial logarithms of ϵ appear at yet higher orders. We find

$$\xi = \tfrac{1}{2}\epsilon^{\epsilon/2d}\left[\epsilon^{3/2} - 0.04916\epsilon^{5/2} - 0.95961\epsilon^{7/2} - \tfrac{3}{8}\epsilon^{9/2}\ln\epsilon + O(\epsilon^{9/2})\right]. \tag{1.7}$$

One may expand

$$\epsilon^{\epsilon/2d} = 1 + \tfrac{1}{8}\epsilon\ln\epsilon + \epsilon^2\left(\tfrac{1}{128}\ln^2\epsilon + \tfrac{1}{32}\ln\epsilon\right) + O(\epsilon^3\ln^3\epsilon) \tag{1.8}$$

if desired, as in Eq. (1.1). If one intends to naively set $\epsilon=1$, this expansion is unnecessary since $\ln\epsilon$ then vanishes and $\epsilon^{\epsilon/2d}=1$ order by order in ϵ. We will comment on the large relative size of the next-to-next-to-leading-order (NNLO) correction at the end of the paper and discuss there the implications of our result for Borel-Padé extrapolations to $d=3$.

In the remainder of this paper, we explain our calculation of ξ to NNLO in the ϵ expansion. In the next section, we briefly review the formalism and diagrammatic rules developed in Ref. [6] for applying the ϵ expansion to this problem. At the beginning of Sec. III, we display the diagrams that need to be evaluated to push the calculation of the effective potential (which is later used to determine ξ) to NNLO in ϵ. Because the efficient evaluation of some diagrams is challenging, we will then take the time to explain our methods in detail. Results for all the diagrams are summarized in Appendix A. In Sec. IV, we put everything together to determine ξ as in Eq. (1.7). Finally, in Sec. V, we explain how the diagrammatic ϵ power counting of Ref. [6] would break down, due to infrared issues, if we proceeded to yet one higher order in ϵ than the calculation reported in this paper. We then show how the proper power counting of ϵ can be restored. Finally, we discuss the implications of our result to extrapolating the value of ξ to $d=3$ in Sec. VI.

II. REVIEW

We will generally follow the conventions and diagrammatic methods of Ref. [6], which we review here. One starts with the Lagrangian

$$\mathcal{L} = \Psi^\dagger\left(i\partial_t + \frac{\nabla^2}{2m}\sigma_3\right)\Psi + \mu\Psi^\dagger\sigma_3\Psi - \frac{1}{c_0}\phi^*\phi + \Psi^\dagger\sigma_+\Psi\phi + \Psi^\dagger\sigma_-\Psi\phi^*, \tag{2.1}$$

where ϕ is a Hubbard-Stratonovich field, $\Psi=(\psi_\uparrow,\psi_\downarrow^\dagger)^\mathsf{T}$ is a two-component Nambu-Gor'kov field, $\sigma_\pm=\frac{1}{2}(\sigma_1\pm i\sigma_2)$, and $\sigma_{1,2,3}$ are the Pauli matrices. The constant c_0 determines the scattering length. In three spatial dimensions,

$$\frac{m}{4\pi a} = -\frac{1}{c_0} + \int\frac{d^3p}{(2\pi)^3}\frac{m}{p^2}. \tag{2.2}$$

The integral on the right hand side of Eq. (2.2) is ultraviolet divergent (and is so in any dimension $d\geq 2$). In a physical system there is always an upper momentum cutoff, for example, the inverse of the range of potential. However, if the system is insensitive to the cutoff, then c_0 should always appear in physical observables in the same combination as in Eq. (2.2), so that observables can be expressed in terms of the scattering length.

Technically, it is cumbersome to carry the integral in Eq. (2.2) across our formulas, so we will use dimensional regularization. The technical advantage of this regularization scheme is that the integral $\int d^dp/p^2$ vanishes in any dimension, and so the connection between c_0 and a becomes very simple. In particular, infinite scattering length corresponds to $c_0=\infty$, so that there is no term quadratic in ϕ in Eq. (2.1). As long as the physics is insensitive to short distances, dimensional regularization will give the same result as other regularization schemes such as a momentum cutoff.[3]

Following Ref. [6], we expand ϕ about its superfluid expectation value $\langle\phi\rangle\equiv\phi_0$ as

$$\phi = \phi_0 + g\varphi, \tag{2.3}$$

where g is chosen to give the dynamics of φ a conventional normalization at leading order in ϵ. In particular, if one computes the small-momentum expansion of the φ self-energy Π of Fig. 1 to leading order in ϵ, one finds

$$\Pi(p_0,\boldsymbol{p}) = \Pi(0) + \frac{g^2m^2}{8\pi^2\epsilon}\left(-p_0 + \frac{p^2}{4m}\right)[1+O(\epsilon)] + O(p_0^2,p^4). \tag{2.4}$$

The choice $g^2m^2=8\pi^2\epsilon[1+O(\epsilon)]$ will then make the momentum dependence above into a conventionally normalized ki-

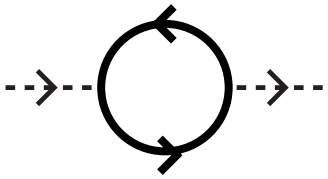

FIG. 1. The one-loop scalar self-energy Π, where solid lines represent Nambu-Gor'kov fermion fields Ψ and dashed lines represent the scalar field variation φ. (There is a similar diagram where one of the external scalar arrows is reversed, mixing φ with φ^*, which we will discuss later and denote $\widetilde{\Pi}$.)

[2]For a textbook overview, see chapters 28 and 41 of Ref. [14].

[3]See Ref. [15] for a standard textbook treatment of dimensional regularization, with emphasis in high-energy physics. For condensed matter applications see, for instance, the textbook treatment in Ref. [14]. For a few examples of use in the theory of cold, dilute atomic gases, see Ref. [16].

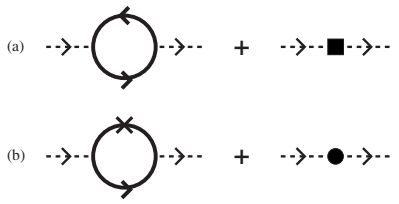

FIG. 2. The rule for using combining divergent subdiagrams with counterterms from $\mathcal{L}_2$ to achieve a simple perturbative expansion in ϵ [6].

netic term for a nonrelativistic particle of mass $M_\varphi=2m$ for $d=4$. Reference [6] found it convenient to define

$$g^2 \equiv \frac{8\pi^2\epsilon}{m^2}\left(\frac{m\phi_0}{2\pi}\right)^{\epsilon/2}. \tag{2.5}$$

Reference [6] then reorganized the Lagrangian in the case of infinite scattering length as a sum $\mathcal{L}=\mathcal{L}_0+\mathcal{L}_1+\mathcal{L}_2$ corresponding to an unperturbed Lagrangian $\mathcal{L}_0$ of a free fermion field Ψ and a free scalar field φ, plus perturbations $\mathcal{L}_1+\mathcal{L}_2$:

$$\mathcal{L}_0 = \Psi^\dagger\left(i\partial_t + \frac{\sigma_3\nabla^2}{2m} + \sigma_+\phi_0 + \sigma_-\phi_0\right)\Psi + \varphi^*\left(i\partial_t + \frac{\nabla^2}{4m}\right)\varphi, \tag{2.6a}$$

$$\mathcal{L}_1 = g\Psi^\dagger\sigma_+\Psi\varphi + g\Psi^\dagger\sigma_-\Psi\varphi^* + \mu\Psi^\dagger\sigma_3\Psi + 2\mu\varphi^*\varphi, \tag{2.6b}$$

$$\mathcal{L}_2 = -\varphi^*\left(i\partial_t + \frac{\nabla^2}{4m}\right)\varphi - 2\mu\varphi^*\varphi. \tag{2.6c}$$

Here, $\mathcal{L}_1$ can be thought of as the interaction terms. As explained in Ref. [6], $\mathcal{L}_2$ should be employed as counterterms to the one-loop diagrams shown in Fig. 2.[4] Feynman rules are shown in Fig. 3, where

$$\hat{\Pi}_0 \equiv -p_0 + \frac{p^2}{4m}. \tag{2.7}$$

(This is our one deviation from the notation of Ref. [6]. We find it convenient to define our $\hat{\Pi}_0$ as the negative of their Π_0. We have added the hat over Π to distinguish it and avoid notational confusion on this point.) The unperturbed propagators generated by $\mathcal{L}_0$ are

[4]The splitup (2.6) might appear unconventional, but the basic idea behind it, as in many other occasions in condensed matter physics, is to resum divergent graphs. The graphs that need to be resummed in our case are multiple insertions of the fermion loop (Fig. 1) into the φ propagator. One could, in principle, formulate a set of Feynman rules where the φ propagator is the inverse of the fermion loop, and fermion loop insertions into the scalar propagator are forbidden by hand. However, the resulting φ propagator would be a very complicated function of momentum and chemical potential. For practical calculations it is much more efficient to give the φ propagator a simpler form, equal to the inverse of the leading $1/\epsilon$ piece of the fermion loop [Eq. (2.4)], and have it corrected in higher loops. To do that at the formal level, the splitup (2.6) is introduced.

vertices

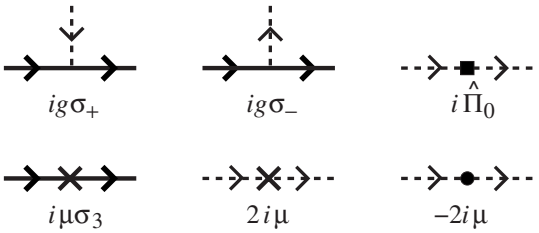

propagators

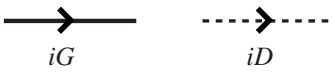

FIG. 3. Feynman rules from Eqs. (2.6) [6].

$$G(p_0,\boldsymbol{p}) = \begin{pmatrix} p_0 - \epsilon_{\boldsymbol{p}} + i\varepsilon & \phi_0 \\ \phi_0 & p_0 + \epsilon_{\boldsymbol{p}} - i\varepsilon \end{pmatrix}^{-1} = \frac{1}{p_0^2 - E_{\boldsymbol{p}}^2 + i\varepsilon}\begin{pmatrix} p_0 + \epsilon_{\boldsymbol{p}} & -\phi_0 \\ -\phi_0 & p_0 - \epsilon_{\boldsymbol{p}} \end{pmatrix} \tag{2.8}$$

and

$$D(p_0,\boldsymbol{p}) = \frac{1}{p_0 - \frac{1}{2}\epsilon_{\boldsymbol{p}} + i\varepsilon}, \tag{2.9}$$

where

$$\epsilon_{\boldsymbol{p}} \equiv \frac{p^2}{2m}, \quad E_{\boldsymbol{p}} \equiv (\epsilon_{\boldsymbol{p}}^2 + \phi_0^2)^{1/2}. \tag{2.10}$$

By analyzing the effective potential $V(\phi_0)$ for the expectation ϕ_0, the minimum is found at $\phi_0 \sim \mu/\epsilon$, or equivalently $\mu \sim \epsilon\phi_0$. The correspondence between the diagrammatic expansion and the ϵ expansion can then be codified by treating ϕ_0 as $O(\epsilon^0)$ and each insertion of μ or g^2 [see Eq. (2.5)] as $O(\epsilon)$. With one exception, this identification gives the relative importance of each diagram of the effective potential to NNLO in the ϵ expansion (the order relevant for the current calculation), provided one uses counterterms according to Fig. 2. The one exception is the one-loop fermion diagram with a single μ insertion, shown in Fig. 4(b), which produces a $1/\epsilon$ that compensates for the μ and which is not canceled by any counterterm diagram.

A word of review is in order regarding the nature of the problem above and below four dimensions. In $d=4-\epsilon$, the corrections to mean-field theory for the unitary Fermi gas are controlled by powers of ϵ. For $d>4$, on the other hand, the problem becomes qualitatively different, as the short distance scale R (the range of the potential) renders the problem non-

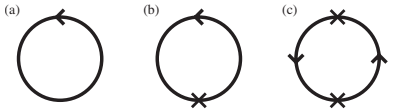

FIG. 4. One-loop diagrams through $O(\epsilon^2)$. Scalar loops are not shown since these vanish due to the retarded nature of the propagators. We will use the notation (a) $V_1^{(0)}$, (b) $V_1^{(\mu)}$, and (c) $V_1^{(\mu\mu)}$.

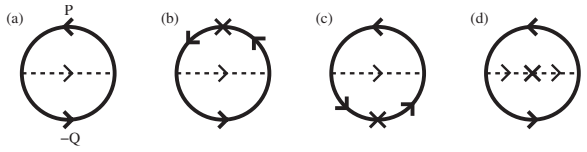

FIG. 5. Two-loop diagrams. The counterterm diagrams for (a–c)—a single scalar loop with an appropriate $\mathcal{L}_2$ counterterm—are not shown because they vanish due to the retarded nature of the scalar propagator. Our notation is (a) $V_2^{(0)}$ and (b–d) $V_2^{(\mu)}$.

universal, and ill defined as $R \to 0$. This is easy to see if one solves the two-body problem in arbitrary dimension, as done by Nussinov and Nussinov [5]. [Precisely at $d=4$, mean-field theory acquires logarithmically small corrections of order $1/\log(L/R)$, where $L \sim n^{-1/3}$ is the typical particle separation.[5]]

III. EVALUATING THE NEXT-TO-NEXT-TO-LEADING-ORDER POTENTIAL

A. The diagrams

Figures 4–6 show the nontrivial diagrams that determine the effective potential $V(\phi_0)$ through NNLO in ϵ, together with our conventions for labeling momenta. In the figure captions, we explain the notation we will use for the contribution of various classes of these diagrams to the effective potential. We have generally not included various one-loop scalar diagrams which vanish simply because of the retarded nature of the scalar propagator D of Eq. (2.9), such as those shown in Fig. 7.[6]

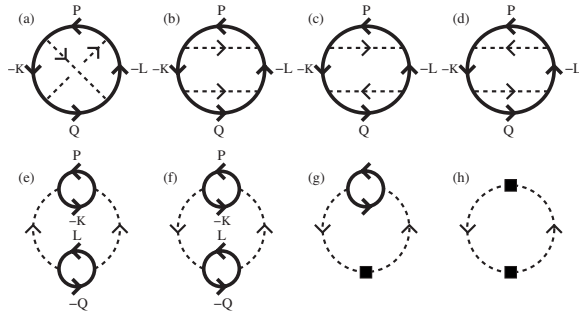

FIG. 6. Three-loop diagrams (including counterterms to bosonic self-energies). (h) vanishes due to the retarded nature of the scalar propagator, but we find it useful to include to make more obvious the cancellation of UV divergences. Our notation is (a) $V_3^{(\otimes)}$, (b–d) $V_3^{(\Sigma\Sigma)}$, (e) $V_3^{(\widetilde{\Pi\Pi})}$, and (f–h) $V_2^{(\Pi\Pi)}$.

B. Cross diagram

As our first example, we will begin by discussing how to efficiently evaluate the contribution $V_3^{(\otimes)}(\phi_0)$ of the cross diagram of Fig. 6(a) to the full effective potential $V(\phi_0)$ at $O(\epsilon^2)$. This is a three-loop diagram and its leading contribution is already $O(\epsilon^2)$ because of the four explicit factors of the coupling g. We may therefore ignore any other ϵ dependence at the order of interest and so can evaluate the loop integrals for exactly $d=4$. (For this diagram, the loop integrals converge for $d=4$, which we will see explicitly.) Our basic approach will be to evaluate all of the frequency integrals. One can then scale all dimensionful parameters out of the remaining momentum integrals. We then perform the dimensionless momentum integrals numerically.

Figure 6(a) gives

$$-iV_3^{(\otimes)} = -(ig)^4 \int_{PQK} iG_{11}(P)iG_{22}(Q)iG_{21}(-K) \times iG_{12}(P+Q+K)iD(P+K)iD(-Q-K), \qquad (3.1)$$

where the overall minus sign on the right-hand side is for the fermion loop. We will use capital letters P to stand for $(p_0,\boldsymbol{p})$, where p_0 is frequency and $\boldsymbol{p}$ is spatial momentum, and we will use the short-hand notations

[5]One can understand this logarithm in the spirit of Nussinov and Nussinov by recalling that the unitary limit corresponds to the presence of a zero-energy bound state, whose wave function will be $\Psi \propto r^{2-d}$ outside of the range R of the potential. The normalization integral $\int d^d r |\Psi|^2 \sim \int d^d r r^{4-2d}$ for the total probability is UV convergent in $d=4-\epsilon$ dimensions, but UV logarithmically divergent in $d=4$ dimensions, where it introduces a logarithmic dependence on R. More technically, if one follows the $d=4-\epsilon$ derivations of Nishida and Son, briefly reviewed here, the source of the small parameters $g^2 \sim \epsilon$ and $\mu/\phi_0 \sim \epsilon$ of the expansion about mean-field theory come from logarithmically divergent (in $d=4$) integrals: respectively, the $1/\epsilon$ in the self-energy (2.4) above [from Fig. 1] and in the potential (4.1) [from Fig. 4(b)]. These integrals $\int d^d p/p^4$ are momentum-space versions of $\int d^d r r^{4-2d}$. Imagine roughly cutting off the integrals in the ultraviolet at the scale $r \sim R$ and $p \sim 1/R$, where the effective theory breaks down and one would need a treatment of the details of the two-body potential. In the calculations of Nishida and Son and in this paper, the infrared is cutoff by the distance scale $s \sim (m\phi_0)^{-1/2}$ associated with the condensate ϕ_0. In $d=4$, we then see that the role of $1/\epsilon$ is replaced by $\ln(s/R)$. (The resulting solution for ϕ_0 will relate s and L by a power of this logarithm, and so $\ln(s/R) \sim \ln(L/R)$ up to corrections suppressed by inverse powers of the logarithm.) We also learn that, in $d=4-\epsilon$ dimensions with ϵ small, R must be exponentially tiny in order to be in the universal regime. Specifically, in order for R not to significantly affect $\int d^d p/p^4$, one must have $R \ll e^{-1/\epsilon} s \sim \epsilon^{1/4} e^{-1/\epsilon} L$.

[6]Naively, these diagrams can be seen to vanish by closing the loop frequency integration in the upper half plane, which contains no poles. There is a technical caveat, however, in that the contribution from the semicircle at infinity cannot be ignored in all cases. This can give ϕ_0-independent contributions to the effective potential which vanish in dimensional regularization and which in other schemes correspond to operator ordering issues, such as whether μ multiplies the Wigner-ordered number operator $\frac{1}{2}(a^\dagger a + a a^\dagger)$ (corresponding to a naive application of the Feynman rules) or the correct normal-ordered operator $a^\dagger a$.

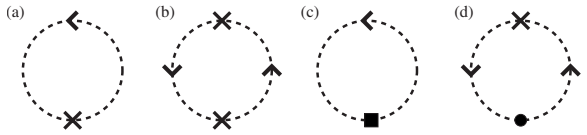

FIG. 7. Examples of diagrams which vanish because of the purely retarded nature of the scalar propagator $D(P)$.

$$\int_P \cdots \equiv \int \frac{dp_0}{2\pi} \frac{d^d p}{(2\pi)^d} \cdots, \quad \int_p \cdots \equiv \int \frac{d^d p}{(2\pi)^d} \cdots . \tag{3.2}$$

Since $G_{21}=G_{12}$, this is the same as

$$V_3^{(\otimes)} = \frac{g^4}{i^3} \int_{PQK} G_{11}(P) G_{22}(Q) G_{12}(-K) G_{12}(P+Q+K) \times D(P+K) D(-Q-K). \tag{3.3}$$

1. The frequency integrals

One could simply use the expressions (2.8) and (2.9) for the propagators and now do the three frequency integrals (p_0, q_0, k_0) by brute force. This approach is tedious and yields complicated expressions with many terms requiring significant effort to simplify. It also naturally produces terms with energy denominators such as $(E_q - E_k + \frac{1}{2}\epsilon_{q+k})^{-1}$ which look like they produce singularities for certain momenta (e.g., $\boldsymbol{q} = -\boldsymbol{k}$ in this example), but all such singularities turn out to cancel between different terms in the final result.

There is, however, a method for carrying out the frequency integration which directly produces much tidier results. The first step is to rewrite

$$G_{11}(P) = \frac{p_0 + \epsilon_p}{p_0^2 - E_p^2 + i\varepsilon} = \frac{1}{2E_p}\left[\frac{E_p + \epsilon_p}{(p_0 - E_p + i\varepsilon)} + \frac{E_p - \epsilon_p}{(p_0 + E_p - i\varepsilon)}\right], \tag{3.4a}$$

$$G_{22}(Q) = \frac{q_0 - \epsilon_q}{q_0^2 - E_q^2 + i\varepsilon} = \frac{1}{2E_q}\left[\frac{E_q - \epsilon_q}{(q_0 - E_q + i\varepsilon)} + \frac{E_q + \epsilon_q}{(q_0 + E_q - i\varepsilon)}\right], \tag{3.4b}$$

$$G_{12}(S) = \frac{-\phi_0}{s_0^2 - E_s^2 + i\varepsilon} = \frac{-\phi_0}{2E_s}\left[\frac{1}{(s_0 - E_s + i\varepsilon)} - \frac{1}{(s_0 + E_s - i\varepsilon)}\right], \tag{3.4c}$$

i.e., to decompose the propagators into retarded and advanced parts. The integrand in Eq. (3.3) then splits into $2^4 = 16$ different terms. We shall see that many of these terms

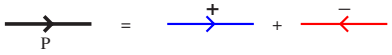

FIG. 8. (Color online) Split of fermion propagators into retarded and advanced terms according to Eq. (3.4).

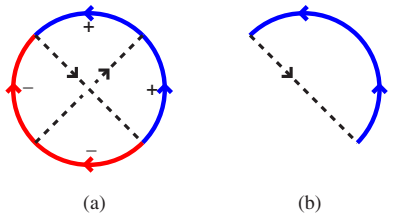

FIG. 9. (Color online) (a) One of the 16 terms generated from Fig. 6(a) by the expansions (3.4). (b) A vanishing loop in this diagram.

trivially vanish, and others are related by symmetry. It is useful to give a graphical depiction of these different terms by schematically rewriting Eqs. (3.4) as in Fig. 8. The first and second terms on the right of this figure denotes the $(p_0 - E_p + i\varepsilon)^{-1}$ and $(p_0 - E_p - i\varepsilon)^{-1}$ terms on the right-hand side of Eqs. (3.4). The + and − signs in Fig. 8 denote the sign of $i\varepsilon$, and the direction of the arrows on the right-hand side of Fig. 8 correspondingly represent the flow of time (forward for a retarded propagator, backward for an advanced one).

In this new notation, Fig. 9(a) shows an example of one of the 2^{16} terms contained in the original diagram of Fig. 6(a). It is easy to see that this term vanishes, because there exists a loop, Fig. 9(b), where all the arrows have the same orientation. If we do that loop integration first, then we can close it in a half plane where there are no poles, and we obtain zero. There are only six terms that do not contain a similar vanishing loop, and they are shown in Fig. 10. The terms represented by the bottom row are related to those of the top row by the change of variables

$$(P, Q, K) \to -(Q, P, K), \tag{3.5}$$

which is a symmetry of the original integrand (3.3).[7] This just represents a change of integration variables, and so the contribution of the second row to the potential will equal that of the first row. We therefore need only evaluate three terms, corresponding to Figs. 10(a)–10(c). Graphically, the operation (3.5) corresponds to flipping the diagrams of Fig. 10 around the horizontal axis and changing the designations $+ \leftrightarrow -$ on the fermion lines.

The next step is to choose combinations of the three frequency integration variables that make the integrals as simple as possible. For each of the terms in Fig. 10, one can find three independent loops that have all arrows but one going around the loop in the same direction. Choose the frequency of the single oppositely oriented line of each such loop to be an integration variable. In Fig. 10, these three frequencies are shown explicitly for each term in the first row, where $l_0 \equiv -(p_0 + q_0 + k_0)$, $u_0 \equiv -(q_0 + k_0)$, and $v_0 \equiv p_0 + k_0$. By closing the frequency integration contours in the appropriate half plane, one can pick up a single pole for each corresponding to the labeled lines in the figure. For instance, from Fig. 10(a), one obtains the term

[7] Another such symmetry is $K \to -(P+Q+K)$ with P and Q unchanged.

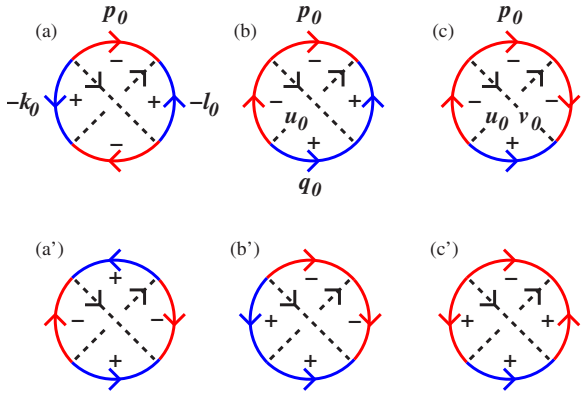

FIG. 10. (Color online) The six nonzero terms of Fig. 6(a) arising from the decomposition (3.4) represented by Fig. 8. The conventions for defining the direction of frequency flow are not given by the arrows here for the fermion lines but by the original diagram of Fig. 6(a) for p_0, q_0, and k_0 and by the definition $l_0=-(p_0+q_0+k_0)$ for l_0.

$$g^4\phi_0^2\int_{pqk}\frac{(E_p-\epsilon_p)(E_q+\epsilon_q)}{2E_p2E_q2E_k2E_{p+q+k}}\int\frac{dp_0}{2\pi i}\frac{dq_0}{2\pi i}\frac{dl_0}{2\pi i}(p_0+E_p-i\varepsilon)^{-1}$$
$$\times(-k_0-E_k+i\varepsilon)^{-1}(-l_0-p_0-k_0+E_q-i\varepsilon)^{-1}(-l_0-E_{p+q+k}$$
$$+i\varepsilon)^{-1}\left(p_0+k_0-\tfrac{1}{2}\epsilon_{p+k}+i\varepsilon\right)^{-1}\left(p_0+l_0-\tfrac{1}{2}\epsilon_{q+k}+i\varepsilon\right)^{-1}, \quad (3.6)$$

which integrates to

$$g^4\phi_0^2\int_{pqk}\frac{(E_p-\epsilon_p)(E_q+\epsilon_q)}{2E_p2E_q2E_k2E_{p+q+k}}(E_p+E_q+E_k+E_{p+q+k})^{-1}$$
$$\times\left(E_p+E_k+\tfrac{1}{2}\epsilon_{p+k}\right)^{-1}\left(E_p+E_{p+q+k}+\tfrac{1}{2}\epsilon_{q+k}\right)^{-1}. \quad (3.7)$$

Doing all the terms of Fig. 10 similarly, we obtain the following result for the contribution of the cross diagram to the effective potential:

$$V_3^{(\otimes)}=g^4\phi_0^2\int_{pqk}\left\{\frac{(E_p-\epsilon_p)}{2E_p2E_q2E_k2E_l\mathcal{S}_{pl}}\left[\frac{(E_q+\epsilon_q)}{\mathcal{S}_{pk}\mathcal{E}_{pqkl}}\right.\right.$$
$$\left.\left.-\frac{(E_q-\epsilon_q)}{\mathcal{T}_{pq,k}}\left(\frac{1}{\mathcal{S}_{pk}}+\frac{1}{\mathcal{S}_{qk}}\right)\right]+(\boldsymbol{p}\leftrightarrow\boldsymbol{q})\right\}, \quad (3.8)$$

where we introduce short-hand notation which will also be convenient for other diagrams:

$$\boldsymbol{l}\equiv-(\boldsymbol{p}+\boldsymbol{q}+\boldsymbol{k}), \quad (3.9a)$$

$$\mathcal{S}_{pk}\equiv E_p+E_k+\tfrac{1}{2}\epsilon_{p+k}, \quad (3.9b)$$

$$\mathcal{T}_{pq,k}\equiv E_p+E_q+\tfrac{1}{2}\epsilon_{p+k}+\tfrac{1}{2}\epsilon_{q+k}, \quad (3.9c)$$

$$\mathcal{E}_{pqkl}\equiv E_p+E_q+E_k+E_l. \quad (3.9d)$$

The $(\boldsymbol{p}\leftrightarrow\boldsymbol{q})$ term at the end of Eq. (3.8) represents the second row of Fig. 10 [using the $(P,Q,K)\rightarrow-(Q,P,K)$ symmetry discussed earlier combined with parity $(\boldsymbol{p},\boldsymbol{q},\boldsymbol{k})\rightarrow-(\boldsymbol{p},\boldsymbol{q},\boldsymbol{k})$]. One may drop the $(\boldsymbol{p}\leftrightarrow\boldsymbol{q})$ in favor of multiplying the rest of the expression by a factor of 2.

Some readers, used to perturbation theory about free Fermi gases, may wonder at the absence of Fermi-sea step functions such as $\theta(\mu-\epsilon_p)$ in the expression (3.8). This is because of the effects of the condensate ϕ_0, which is large compared to the chemical potential $\mu\sim\epsilon\phi_0$. The system is not describable as a small perturbation to a free Fermi sea. In Appendix B, we give a brief, illustrative example of what happens to a standard $\theta(\mu-\epsilon_p)$ factor if one adds a condensate ϕ_0 and increases it to $\phi_0\gg\mu$.

2. The momentum integrals

The remaining integrals (3.8) that we need to do can be made dimensionless by rescaling momenta as

$$\boldsymbol{p}\rightarrow(2m\phi_0)^{1/2}\boldsymbol{p}, \quad (3.10)$$

which has the effect of replacing $g^4\phi_0^2$ by $g^4\phi_0^{-3}(2m\phi_0)^{3d/2}$ outside the integral and replacing ϵ_p and E_p by the dimensionless versions

$$\bar{\epsilon}_p\equiv p^2,\quad \bar{E}_p\equiv(p^4+1)^{1/2} \quad (3.11)$$

everywhere inside the integral. Using the formula (2.5) for g^2, this can be written as

$$V_3^{(\otimes)}=\phi_0\left(\frac{m\phi_0}{2\pi}\right)^{d/2}\epsilon^2\mathcal{K}_3^{(\otimes)}(\epsilon), \quad (3.12)$$

where

$$\mathcal{K}_3^{(\otimes)}(\epsilon)\equiv 4(4\pi)^{3d/2}\int_{pqk}\frac{2(\bar{E}_p-\bar{\epsilon}_p)}{2\bar{E}_p2\bar{E}_q2\bar{E}_k2\bar{E}_l\bar{\mathcal{S}}_{pl}}\left[\frac{(\bar{E}_q+\bar{\epsilon}_q)}{\bar{\mathcal{S}}_{pk}\bar{\mathcal{E}}_{pqkl}}\right.$$
$$\left.-\frac{(\bar{E}_q-\bar{\epsilon}_q)}{\bar{\mathcal{T}}_{pq,k}}\left(\frac{1}{\bar{\mathcal{S}}_{pk}}+\frac{1}{\bar{\mathcal{S}}_{qk}}\right)\right] \quad (3.13)$$

is a dimensionless function of ϵ. For a NNLO evaluation of the potential, we may evaluate $\mathcal{K}_3^{(\otimes)}$ at $\epsilon=0$, so that

$$V_3^{(\otimes)}=\phi_0\left(\frac{m\phi_0}{2\pi}\right)^{d/2}\epsilon^2[K_3^{(\otimes)}+O(\epsilon)], \quad (3.14)$$

where the numerical constant $K_3^{(\otimes)}$ is the result of the integral (3.13) evaluated in exactly four dimensions.

For numerical evaluation, we use rotational invariance to rewrite the momentum integrals as a six-dimensional integral over the magnitudes of and angles between the momenta:

$$\int\frac{d^4p}{(2\pi)^4}\frac{d^4q}{(2\pi)^4}\frac{d^4k}{(2\pi)^4}=\frac{1}{(2\pi)^8}\int_0^\infty p^3q^3k^3dpdqdk\int_0^\pi\sin^2\theta_p\sin^2\theta_q\sin\xi_q d\theta_p d\theta_q d\xi_q, \quad (3.15)$$

corresponding to a choice of Cartesian coordinates aligned so that

$$\boldsymbol{k} = k(1,0,0,0), \tag{3.16a}$$

$$\boldsymbol{p} = p(\cos\,\theta_p, \sin\,\theta_p, 0, 0), \tag{3.16b}$$

$$\boldsymbol{q} = q(\cos\,\theta_q, \sin\,\theta_q \cos\,\xi_q, \sin\,\theta_q \sin\,\xi_q, 0). \tag{3.16c}$$

We then perform the integral (3.13) numerically using adaptive Monte Carlo integration. The result is

$$K_3^{(\otimes)} \simeq 0.15101, \tag{3.17}$$

where $\simeq$ in this paper will mean that the result has an estimated error of at most ±1 in the last digit. Equations (3.14) and (3.17) represent our final result for the cross diagram of Fig. 6(a).

C. Basic two-loop diagram through $O(\epsilon^2)$

The basic two-loop diagram of Fig. 5(a) is given by

$$-iV_2^{(0)} = -(ig)^2 \int_{PQ} iG_{11}(P) iG_{22}(-Q) iD(P+Q). \tag{3.18}$$

Doing the frequency integrals,

$$V_2^{(0)} = -g^2 \int_{\boldsymbol{pq}} \frac{(E_p - \epsilon_p)(E_q - \epsilon_q)}{2E_p 2E_q \mathcal{S}_{pq}}. \tag{3.19}$$

Rescaling momenta as in Eq. (3.10),

$$V_2^{(0)} = \phi_0 \left(\frac{m\phi_0}{2\pi}\right)^{d/2} \epsilon \mathcal{K}_2(\epsilon) \tag{3.20}$$

with

$$\mathcal{K}_2(\epsilon) = -2(4\pi)^d \int_{\boldsymbol{pq}} \frac{(\bar{E}_p - \bar{\epsilon}_p)(\bar{E}_q - \bar{\epsilon}_q)}{2\bar{E}_p 2\bar{E}_q \bar{\mathcal{S}}_{pq}}, \tag{3.21}$$

If one sets $d=4$, one has $\mathcal{K}_2(0) = -C_2$ where

$$C_2 \equiv 2(4\pi)^4 \int \frac{d^4p}{(2\pi)^4} \frac{d^4q}{(2\pi)^4} \frac{(\bar{E}_p - \bar{\epsilon}_p)(\bar{E}_q - \bar{\epsilon}_q)}{2\bar{E}_p 2\bar{E}_q \bar{\mathcal{S}}_{pq}}, \tag{3.22}$$

which gives

$$C_2 \simeq 0.14424 \tag{3.23}$$

upon numerical integration, all just as in Ref. [6]. For a NNLO calculation of the potential, however, we need the next term in the expansion of $\mathcal{K}_2(\epsilon)$ in ϵ. We can obtain this by rewriting the d dimensional integration as

$$\int \frac{d^dp}{(2\pi)^d} \frac{d^dq}{(2\pi)^d} = \frac{8}{(4\pi)^{d+\frac{1}{2}} \Gamma\left(\frac{d}{2}\right) \Gamma\left(\frac{d-1}{2}\right)} \int_0^\infty p^{d-1} q^{d-1} dp dq \int_0^\pi \sin^{d-2}\,\theta_{pq} d\theta_{pq}, \tag{3.24}$$

where θ_{pq} is the angle between $\boldsymbol{p}$ and $\boldsymbol{q}$, and then expanding in ϵ. The result is

$$\mathcal{K}_2(\epsilon) = -\left[1 + \left(\tfrac{3}{2} - \gamma - \ln 2\right)\epsilon\right] C_2 + \epsilon C_2^{(\log)} + O(\epsilon^2) \tag{3.25}$$

where

$$C_2^{(\log)} = 2(4\pi)^4 \int \frac{d^4p}{(2\pi)^4} \frac{d^4q}{(2\pi)^4} \frac{(\bar{E}_p - \bar{\epsilon}_p)(\bar{E}_q - \bar{\epsilon}_q)}{2\bar{E}_p 2\bar{E}_q \bar{\mathcal{S}}_{pq}} \times \ln(|\boldsymbol{p}||\boldsymbol{q}| \sin\,\theta_{pq}), \tag{3.26a}$$

with numerical value

$$C_2^{(\log)} \simeq 0.14238. \tag{3.26b}$$

D. Scalar loop with two self-energy insertions

The next diagrams we consider are those of Figs. 6(f)–6(h), which correspond to a scalar loop with two self-energy insertions Π and the corresponding counterterm diagrams. Individually, the diagrams of Figs. 6(f) and 6(g) are ultraviolet (UV) divergent; it is only in their combination that the divergences are eliminated. So we must be careful not to set $d=4$ in integrations until we have organized the terms into absolutely convergent integrals. We will keep d general in what follows until near the end.

Together, Figs. 6(f)–6(h) give

$$-iV_3^{(\Pi\Pi)} = \tfrac{1}{2} \int_V [iD(V)]^2 \{-i[\Pi(V) - \hat{\Pi}_0(V)]\}^2, \tag{3.27}$$

where $V=(v_0, \boldsymbol{v})$ is the frequency and momentum of the scalar line, Π is the one-loop scalar self-energy given by

$$-i\Pi(V) = -(ig)^2 \int_P iG_{11}(P) iG_{22}(P-V), \tag{3.28}$$

and the corresponding counterterm $\hat{\Pi}_0$ is given by Eq. (2.7).

The frequency integral in Eq. (3.28) is straightforward, especially using Eq. (3.4), yielding

$$\Pi(V) = g^2 \int_p \frac{1}{2E_p 2E_{p-v}} \left[\frac{(E_p + \epsilon_p)(E_{p-v} + \epsilon_{p-v})}{v_0 - E_p - E_{p-v} + i\varepsilon} - \frac{(E_p - \epsilon_p)(E_{p-v} - \epsilon_{p-v})}{v_0 + E_p + E_{p-v} - i\varepsilon} \right]. \tag{3.29}$$

The momentum integral would be UV divergent if we set $d=4$. We will isolate this divergence by isolating the large $\boldsymbol{p}$ behavior of the integrand by writing

$$\Pi(V) = \Pi_{\rm div}(V) + \Pi_{\rm reg}(V), \tag{3.30}$$

where the divergent piece of the momentum integral is

$$\Pi_{\rm div}(V) \equiv g^2 \int_p \frac{1}{v_0 - \epsilon_p - \epsilon_{p-v} + i\varepsilon}, \tag{3.31}$$

and the remainder is

$$\Pi_{\rm reg}(V) = g^2 \int_p \left\{ \frac{1}{2E_p 2E_{p-v}} \left[\frac{(E_p + \epsilon_p)(E_{p-v} + \epsilon_{p-v})}{v_0 - E_p - E_{p-v} + i\varepsilon} - \frac{(E_p - \epsilon_p)(E_{p-v} - \epsilon_{p-v})}{v_0 + E_p + E_{p-v} - i\varepsilon} \right] - \frac{1}{v_0 - \epsilon_p - \epsilon_{p-v} + i\varepsilon} \right\}. \tag{3.32}$$

The strategy here is to have chosen the form of $\Pi_{\rm div}$ to be simple enough that we can manage to evaluate the integral in general dimension d. The result of evaluating Eq. (3.31) is[8]

$$\Pi_{\rm div}(V) = -g^2 \Gamma\left(1 - \tfrac{d}{2}\right) \left(\frac{m}{4\pi}\right)^{d/2} \left(-v_0 + \tfrac{1}{2}\epsilon_{\boldsymbol{v}} - i\varepsilon\right)^{d/2-1} = -\frac{\epsilon}{2} \Gamma\left(1 - \tfrac{d}{2}\right) \left(-v_0 + \tfrac{1}{2}\epsilon_{\boldsymbol{v}}\right) \left(\frac{-v_0 + \frac{1}{2}\epsilon_{\boldsymbol{v}} - i\varepsilon}{2\phi_0} \right)^{-\epsilon/2}, \tag{3.33}$$

where Eq. (2.5) has been used for g^2. Now use our split (3.30) of Π to rewrite the contribution to the potential given by Eq. (3.27) as

$$V_3^{(\rm III)} = -\frac{1}{2i} \int_V [D(V)]^2 \{ [\Pi_{\rm reg}(V)]^2 + 2\Pi_{\rm reg}(V)[\Pi_{\rm div}(V) - \hat{\Pi}_0(V)] + [\Pi_{\rm div}(V) - \hat{\Pi}_0(V)]^2 \}. \tag{3.34}$$

In dimensional regularization, the terms which do not involve $\Pi_{\rm reg}$ integrate to zero because of their scaling properties. For example, changing integration variables

$$(v_0, \boldsymbol{v}) \to (\lambda^2 v_0, \lambda \boldsymbol{v}) \tag{3.35}$$

for an arbitrary constant λ,

$$\int \frac{dv_0}{2\pi} \frac{d^d v}{(2\pi)^d} [D(V)]^2 [\Pi_{\rm div}(V)]^2 = \int \frac{\lambda^2 dv_0}{2\pi} \frac{\lambda^d d^d v}{(2\pi)^d} [\lambda^{-2} D(V)]^2 [\lambda^{d-2} \Pi_{\rm div}(V)]^2. \tag{3.36}$$

So this integral must equal itself times $\lambda^{3(d-2)}$ and so must vanish. For similar reasons, we may dispense which each term generated by expanding the square in

$$-\frac{1}{2i} \int_V [D(V)]^2 [\Pi_{\rm div}(V) - \hat{\Pi}_0(V)]^2 = 0.$$

For the first term in Eq. (3.34), we continue by performing the v_0 integration, using Eq. (3.32) for $\Pi_{\rm reg}$. One may avoid the bother of dealing with the double pole from $D(K)$ by closing in the upper-half plane. The result is

$$-\frac{1}{2i} \int_V [D(V)]^2 [\Pi_{\rm reg}(V)]^2 = -\frac{g^4}{2} \int_{pqk} \left\{ \frac{(E_p - \epsilon_p)(E_k - \epsilon_k)}{2E_p 2E_q 2E_k 2E_l \mathcal{S}_{pk}^2} \left[\frac{(E_q - \epsilon_q)(E_l - \epsilon_l)}{\mathcal{S}_{ql}} + \frac{(E_q + \epsilon_q)(E_l + \epsilon_l)}{\mathcal{E}_{pqkl}} - \frac{2E_q 2E_l}{(E_p + \epsilon_q + E_k + \epsilon_l)} \right] + (\boldsymbol{pk} \leftrightarrow \boldsymbol{ql}) \right\}, \tag{3.37}$$

where we have used the notation of Eqs. (3.9) and the momentum naming conventions shown in Fig. 6(f) (so $\boldsymbol{v}=\boldsymbol{p}+\boldsymbol{k}$). This integral is absolutely convergent in $d=4$, and so we may evaluate it numerically just as we did for the cross diagram in Sec. III B 2, giving

$$-\frac{1}{2i} \int_V [D(V)]^2 [\Pi_{\rm reg}(V)]^2 = \phi_0 \left(\frac{m\phi_0}{2\pi} \right)^{d/2} \epsilon^2 [K_3^{(\rm III,1)} + O(\epsilon)] \tag{3.38}$$

with

[8] The dependence of Eq. (3.33) only on the combination $-v_0 + \frac{1}{2}\epsilon_{\boldsymbol{v}}$ is a result of Galilean invariance. Galilean invariance is broken by the condensate ϕ_0, but ϕ_0 does not appear in our definition of $\Pi_{\rm div}$.

$$K_3^{(\mathrm{III},1)} \simeq 0.006\,753. \tag{3.39}$$

Finally, we need the second term from the right-hand side of Eq. (3.34). Taking Π_{reg} and Π_{div} from Eqs. (3.32) and (3.33), and closing the v_0 integration in the upper half plane to avoid the branch cut in Π_{div}, one finds

$$\begin{aligned} -\frac{1}{i}\int_V [D(V)]^2\Pi_{\mathrm{reg}}(V)[\Pi_{\mathrm{div}}(V)-\hat{\Pi}_0(V)] &= g^2\int_{pk}\frac{(E_p-\epsilon_p)(E_k-\epsilon_k)}{2E_p 2E_k \mathcal{S}_{pk}^2}[\Pi_{\mathrm{div}}(V)-\hat{\Pi}_0(V)]\Big|_{-v_0+\frac{1}{2}\epsilon_v=S_{pk}} \\ &= g^2\int_{pk}\frac{(E_p-\epsilon_p)(E_k-\epsilon_k)}{2E_p 2E_k \mathcal{S}_{pk}}\left[-\frac{\epsilon}{2}\Gamma\left(1-\tfrac{d}{2}\right)\left(\frac{S_{pk}}{2\phi_0}\right)^{-\epsilon/2}-1\right]. \end{aligned} \tag{3.40}$$

If we expand about four dimensions, we obtain absolutely convergent integrals at every order in ϵ. We are therefore free to expand the integrand in ϵ to obtain

$$[1+O(\epsilon)]\frac{\epsilon g^2}{2}\int_{pk}\frac{(E_p-\epsilon_p)(E_k-\epsilon_k)}{2E_p 2E_k \mathcal{S}_{pk}}\left[1-\gamma-\ln\left(\frac{S_{pk}}{2\phi_0}\right)\right]. \tag{3.41}$$

Rescaling momenta in the usual way then gives

$$\begin{aligned} &-\frac{1}{i}\int_V [D(V)]^2\Pi_{\mathrm{reg}}(V)[\Pi_{\mathrm{div}}(V)-\hat{\Pi}_0(V)] \\ &\quad=\phi_0\left(\frac{m\phi_0}{2\pi}\right)^{d/2}\left\{\left[\tfrac{1}{2}(1-\gamma+\ln 2)C_2-C_2^{(\log,\mathcal{S})}\right]\epsilon^2+O(\epsilon^3)\right\} \end{aligned} \tag{3.42}$$

with C_2 given by Eqs. (3.22) and (3.23),

$$C_2^{(\log,\mathcal{S})} \equiv 2(4\pi)^4\int\frac{d^4p}{(2\pi)^4}\frac{d^4q}{(2\pi)^4}\frac{(\bar{E}_p-\bar{\epsilon}_p)(\bar{E}_q-\bar{\epsilon}_q)}{2\bar{E}_p 2\bar{E}_q \bar{\mathcal{S}}_{pq}}\tfrac{1}{2}\ln(\bar{\mathcal{S}}_{pq}) \tag{3.43a}$$

giving

$$C_2^{(\log,\mathcal{S})} \simeq 0.194\,08. \tag{3.43b}$$

Our final result for the contribution of Figs. 6(f)–6(h) to the effective potential is the sum of Eqs. (3.38) and (3.42):

$$\begin{aligned} V_3^{(\mathrm{III})} = \phi_0\left(\frac{m\phi_0}{2\pi}\right)^{d/2}\Big\{\Big[K_3^{(\mathrm{III},1)}+\tfrac{1}{2}(1-\gamma+\ln 2)C_2 \\ -C_2^{(\log,\mathcal{S})}\Big]\epsilon^2+O(\epsilon^3)\Big\}. \end{aligned} \tag{3.44}$$

E. Remaining diagrams

The remaining diagrams are relatively easy, and we summarize results in Appendix A. Here, we will just make a few comments on method.

A simple way to handle diagrams with self-energy insertions is to consider the diagram without any such insertions, and then replace ϵ_p by $\epsilon_p^\mu \equiv \epsilon_p - \mu$ in both ϵ_p and $E_p=(\epsilon_p^2+\phi_0^2)^{1/2}$ for fermion energies, and replace $\frac{1}{2}\epsilon_v$ by $\frac{1}{2}\epsilon_v - 2\mu$ for boson energies. For instance, to simultaneously evaluate all of the two-loop diagrams of Figs. 5(b)–5(d) with chemical potential insertions, replace Eq. (3.19) for the basic two-loop result $V_2^{(0)}$ by

$$-g^2\int_{pq}\frac{(E_p^\mu-\epsilon_p^\mu)(E_q^\mu-\epsilon_q^\mu)}{2E_p^\mu 2E_q^\mu\left(E_p^\mu+E_q^\mu+\frac{1}{2}\epsilon_{p+q}-2\mu\right)}, \tag{3.45}$$

where $E_p^\mu \equiv [(\epsilon_p-\mu)^2+\phi_0^2]^{1/2}$. Then Taylor expand the integrand to the desired order in μ, which in this case is first order. The same method can be used on the one-loop integrals of Fig. 4 starting from the basic one-loop integral of Fig. 4(a), [9]

$$V_1^{(0)} = i\int_P \ln\det[-iG^{-1}(P)] = -\int_p E_p. \tag{3.46}$$

IV. RESULT FOR ξ

Combining the results given previously and in Appendix A, the full effective potential at NNLO in ϵ is

$$\begin{aligned} V(\phi_0) = \left(\frac{m\phi_0}{2\pi}\right)^{d/2}\Big[\frac{\phi_0}{3}(1+a_1\epsilon+a_2\epsilon^2)-\frac{\mu}{\epsilon}(1+b_1\epsilon+b_2\epsilon^2) \\ -\frac{\mu^2}{2\phi_0}\Big]+O(\epsilon^3), \end{aligned} \tag{4.1}$$

where ϕ_0 is treated as $O(1)$ and μ as $O(\epsilon)$. The various numerical coefficients are

$$a_1 = \tfrac{1}{2}\left(\tfrac{7}{3}-\gamma-\ln 2\right)-3C_2 \simeq 0.098\,77, \tag{4.2}$$

$$\begin{aligned} a_2 = \tfrac{1}{8}\left(\tfrac{7}{3}-\gamma-\ln 2\right)^2+\tfrac{19}{72}+3\Big[\left(-1+\tfrac{1}{2}\gamma+\tfrac{3}{2}\ln 2\right)C_2+C_2^{(\log)} \\ -C_2^{(\log,\mathcal{S})}+K_3\Big] \simeq -0.158\,40, \end{aligned} \tag{4.3}$$

$$b_1 = \tfrac{1}{2}\left(\tfrac{1}{2}-\gamma+\ln 2\right) \simeq 0.307\,97, \tag{4.4}$$

[9] There are similar issues as footnote 6 concerning the frequency integral and the behavior of its integrand at infinity. In general regularization schemes, this could be avoided by defining the integrals here with ϕ_0 (and μ) independent subtractions, which will not affect the determination of ξ from the effective potential: $i\int_P\{\ln\det[-iG^{-1}(P;\phi_0)]-\ln\det[-iG^{-1}(P;0)]\}=-\int_p(E_p-\epsilon_p)$. But, in dimensional regularization, the subtracted term vanishes anyway by scaling arguments similar to those reviewed in Sec. III D.

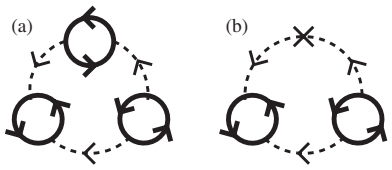

FIG. 11. Two examples of diagrams that produce logarithmic infrared divergences.

$$b_2 = \tfrac{1}{8}\left(\tfrac{1}{2} - \gamma + \ln 2\right)^2 + \tfrac{1}{32} - K_2^{(\mu)} \simeq 0.337\,03, \quad (4.5)$$

where

$$K_3 \equiv K_3^{(\otimes)} + K_3^{(\mathrm{III},1)} + K_3^{(\Sigma\Sigma)} + K_3^{(\widetilde{\mathrm{III}})} \simeq -0.183\,48. \quad (4.6)$$

The ratio ξ can be computed from $V(\phi_0,\mu)$ by the procedure used in Ref. [6]. First, we determine the expectation ϕ_0 which minimizes the potential:

$$\phi_0 = \frac{2\mu}{\epsilon}[1 + 0.125\,86\epsilon + 0.568\,45\epsilon^2 + O(\epsilon^3)]. \quad (4.7)$$

Then we determine the fermion number density n from the pressure $P=-V(\phi_0)$, giving

$$n = \frac{\partial P}{\partial \mu} = -\frac{\partial V}{\partial \mu} = \frac{1}{\epsilon}\left(\frac{m\phi_0}{2\pi}\right)^{d/2}\left[1 + b_1\epsilon + b_2\epsilon^2 + \frac{\epsilon\mu}{\phi_0} + O(\epsilon^3)\right]. \quad (4.8)$$

Next, we take the formula for the Fermi energy $\epsilon_F(n)$ of a d-dimensional ideal Fermi gas with the same density,

$$\epsilon_F = \frac{2\pi}{m}\left[\tfrac{1}{2}\Gamma\left(\tfrac{d}{2}+1\right)n\right]^{2/d}. \quad (4.9)$$

For the density (4.8), this then gives

$$\xi \equiv \frac{\mu}{\epsilon_F} = \frac{\epsilon^{2/d}\mu}{\phi_0}\left\{\tfrac{1}{2}\Gamma\left(\tfrac{d}{2}+1\right)\left[1 + b_1\epsilon + b_2\epsilon^2 + \frac{\epsilon\mu}{\phi_0} + O(\epsilon^3)\right]\right\}^{-2/d}. \quad (4.10)$$

Substituting in the expectation (4.7) for ϕ_0, and rewriting $\epsilon^{2/d} = \epsilon^{\epsilon/2d}\epsilon^{1/2}$, produces the final result (1.7) through NNLO. The additional logarithmic term shown in Eq. (1.7) at the order beyond NNLO is the subject of the next section.

V. THE ϵ EXPANSION BEYOND NEXT-TO-NEXT-TO-LEADING-ORDER

A. General

In this section, we discuss a difficulty that arises in applying the diagrammatic expansion of Sec. II if one were to proceed to yet one higher order in ϵ, attempting to evaluate the effective potential through $O(\epsilon^3)$ [and so ξ through $O(\epsilon^{9/2})$]. The problem is an infrared problem arising from the fact that the scalar excitations, unlike the fermionic excitations, are not gapped.

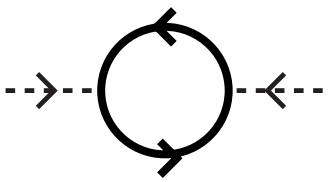

FIG. 12. The self-energy $\widetilde{\Pi}$ that mixes φ with φ^*.

For the sake of specificity, consider the $O(\epsilon^3)$ contribution to the effective potential made by the diagram of Fig. 11(a). Together with the corresponding counterterm diagram, this gives a contribution to the effective potential

$$V_4^{(\mathrm{example})} = -\frac{1}{i}\int_V [D(V)]^2 D(-V)[\Pi(V) - \hat{\Pi}_0(V)][\widetilde{\Pi}(V)]^2, \quad (5.1)$$

where the one-loop self-energy Π is given by Fig. 1 and $\widetilde{\Pi}$ by Fig. 12. Let us now explore the contribution to this integral from small scalar frequency and momentum: $|v_0| \ll \phi_0$ and $\frac{1}{2}\epsilon_{\boldsymbol{v}} \ll \phi_0$. At small V, we approximate V as zero inside the self-energies, and this region of integration contributes

$$V_4^{(\mathrm{ex,small}\ V)} \sim -\Pi(0)[\widetilde{\Pi}(0)]^2 \frac{1}{i}\int_V [D(V)]^2 D(-V), \quad (5.2)$$

where the integration is restricted to small V. [Note that $\hat{\Pi}_0(0)=0$.] The frequency integral is simple, giving

$$V_4^{(\mathrm{ex,small}\ V)} \sim \Pi(0)[\widetilde{\Pi}(0)]^2 \int_{\boldsymbol{v}} \frac{1}{\epsilon_{\boldsymbol{v}}^2}. \quad (5.3)$$

The momentum integral is IR divergent in $d \leq 4$. So our evaluation of diagrams has broken down in the infrared if $\Pi(0)$ and $\widetilde{\Pi}(0)$ are nonzero.[10]

Another example of a diagram producing similar problems is shown in Fig. 11(b). Adding one or more additional self-energy or chemical potential insertions to the scalar loop in either diagram would generate even more severe (power-law) infrared divergences.

[10] If one blindly tried to regulate the IR divergences using dimensional regularization (which we have previously used only to regulate the UV), then the IR momentum integral in Eq. (5.3) would generate a factor of $1/\epsilon$, which would in any case destroy the ϵ counting of Sec. II. The integral does not generate zero (by scaling arguments like those of Sec. III D) because the $1/\epsilon_{\boldsymbol{v}}^2$ integrand is an approximation valid only for $|\boldsymbol{v}| \ll \phi_0$. The behavior of the full result changes for $|\boldsymbol{v}| \gtrsim \phi_0$, and so ϕ_0 provides a scale. (We say "blindly tried to regulate" because dimensional regularization throws away nonlogarithmic divergences, and it does not distinguish between IR and UV logarithmic divergences. This means it can be a dangerous procedure unless you already know that all divergences will cancel in the final result.)

We shall see in a moment that $\Pi(0)$ and $\widetilde{\Pi}(0)$ are both $O(\mu)$. The problem, then, is that when $\boldsymbol{v}$ is small enough that $\epsilon_{\boldsymbol{v}}$ is of order $\mu \ll \phi_0$, it is no longer a good approximation to treat the scalar self-energies, or the chemical potential 2μ, as perturbations to $D^{-1}=-v_0+\frac{1}{2}\epsilon_{\boldsymbol{v}}$. One must therefore resum $\Pi(0)$, $\widetilde{\Pi}(0)$, and 2μ into scalar propagators in order to recover a well-behaved perturbation theory. Equivalently, one must use the appropriate low-energy scalar effective theory when evaluating the contribution of low-energy scalars ($|v_0| \ll \phi_0$) to the effective potential. At low energy, the effective scalar propagator would be generated by the effective interactions

$$\mathcal{L}_{\text{eff}} \simeq \varphi^*\left(i\partial_t + \frac{\nabla^2}{4m}\right)\varphi + 2\mu\varphi^*\varphi - \Pi(0)\varphi^*\varphi - \widetilde{\Pi}(0)\tfrac{1}{2}(\varphi\varphi + \varphi^*\varphi^*) \equiv \tfrac{1}{2}\begin{pmatrix}\varphi\\ \varphi^*\end{pmatrix}^\dagger \mathcal{D}^{-1}\begin{pmatrix}\varphi\\ \varphi^*\end{pmatrix}, \tag{5.4}$$

with corresponding propagator

$$\mathcal{D}(P) = \begin{pmatrix} p_0 - \frac{1}{2}\epsilon_{\boldsymbol{p}} + 2\mu - \Pi(0) + i\varepsilon & -\widetilde{\Pi}(0) \\ -\widetilde{\Pi}(0) & -p_0 - \frac{1}{2}\epsilon_{\boldsymbol{p}} + 2\mu - \Pi(0) + i\varepsilon \end{pmatrix}^{-1}. \tag{5.5}$$

To better understand the structure of this propagator, we now evaluate $\Pi(0)$ and $\widetilde{\Pi}(0)$. From Eq. (3.29),

$$\Pi(0) = -g^2 \int_p \frac{E_{\boldsymbol{p}}^2 + \epsilon_{\boldsymbol{p}}^2}{4E_{\boldsymbol{p}}^3}. \tag{5.6}$$

$\widetilde{\Pi}(0)$ is given by

$$\widetilde{\Pi}(0) = \frac{g^2}{i}\int_P [G_{12}(P)]^2 = g^2 \int_p \frac{\phi_0^2}{4E_{\boldsymbol{p}}^3}. \tag{5.7}$$

In dimensional regularization, the momentum integrals give

$$\Pi(0) = -\frac{g^2}{\phi_0}\left(\frac{m\phi_0}{4\pi}\right)^{d/2}\frac{\left(1+\frac{d}{2}\right)\Gamma\left(\frac{1}{2}-\frac{d}{4}\right)}{4\Gamma\left(\frac{1}{2}+\frac{d}{4}\right)} = 3\mu[1+O(\epsilon)] \tag{5.8}$$

and

$$\widetilde{\Pi}(0) = \frac{(d-2)}{(d+2)}\Pi(0) = \mu[1+O(\epsilon)], \tag{5.9}$$

where we have used Eqs. (2.5) and (4.7) for g^2 and ϕ_0. To leading order in ϵ for scalars with energy of order μ, the effective low-energy interactions (5.4) are then

$$\mathcal{L}_{\text{eff}} \simeq \varphi^*\left(i\partial_t + \frac{\nabla^2}{4m}\right)\varphi - \tfrac{1}{2}\mu(\varphi+\varphi^*)^2 \tag{5.10}$$

with

$$\mathcal{D}(P) = \begin{pmatrix} p_0 - \frac{1}{2}\epsilon_{\boldsymbol{p}} - \mu + i\varepsilon & -\mu \\ -\mu & -p_0 - \frac{1}{2}\epsilon_{\boldsymbol{p}} - \mu + i\varepsilon \end{pmatrix}^{-1}. \tag{5.11}$$

The imaginary part of φ remains gapless, which must occur in any consistent approximation since it corresponds to a Goldstone boson.

With this formula, we can now compute the leading contribution to the effective potential from low-energy scalars and see that all is well. Analogous to the fermionic result (3.46), it is

$$V^{(\text{soft }\varphi)} \simeq -\frac{i}{2}\int_P \ln\det[-i\mathcal{D}^{-1}(P)] = -\frac{i}{2}\int_P \ln\left[p_0^2 - \tfrac{1}{2}\epsilon_{\boldsymbol{p}}\left(\tfrac{1}{2}\epsilon_{\boldsymbol{p}} + 2\mu\right) + i\varepsilon\right] = \frac{1}{2}\int_{\boldsymbol{p}}\left[\tfrac{1}{2}\epsilon_{\boldsymbol{p}}\left(\tfrac{1}{2}\epsilon_{\boldsymbol{p}} + 2\mu\right)\right]^{1/2}. \tag{5.12}$$

This integral has no infrared divergences. If we naively expanded the integrand in powers of μ, we would obtain infrared divergences starting at third order $\sim\mu^3\int_{\boldsymbol{p}}\epsilon_{\boldsymbol{p}}^{-2}$. This is the same order as the result (5.3) for Fig. 11 that started this discussion. If we instead integrate Eq. (5.12) up to a UV momentum cutoff $(4m\Lambda)^{1/2}$ for the effective theory, we find an expansion in μ of the form

$$V^{(\text{soft }\varphi)} \simeq m^2\left[\#\Lambda^3 + \#\mu\Lambda^2 + \#\mu^2\Lambda + \#\mu^3\ln\left(\frac{\mu}{\Lambda}\right) + \#\mu^3 + \cdots\right]. \tag{5.13}$$

The soft effective scalar theory breaks down at $\epsilon_{\boldsymbol{p}} \gtrsim \phi_0$, so one should very roughly think of the energy scale Λ as of order ϕ_0.

The moral of this story is that one will have to make a proper treatment of low-energy scalar fields in order to go to higher orders in ϵ than the NNLO calculation performed in the bulk of this paper. In particular, the approach of Sec. II would lead to logarithmic divergences in the effective potential at $O(\epsilon^3)$ and worse divergences at higher order, but a proper resummation of soft scalar physics will resolve these divergences into $O(\mu^3\ln(\mu/\phi_0)) = O(\epsilon^3\ln\epsilon)$. This corresponds to a correction to ξ of order $\epsilon^{\epsilon/2d}\epsilon^{9/2}\ln\epsilon$.

B. The coefficient of the logarithm

Though we are not prepared to make a full calculation of the order beyond NNLO in the ϵ expansion, it is simple to extract the coefficient of the logarithm at that order from the preceding discussion. Naively expand the integrand in the formula (5.12) for the soft contribution $V^{(\text{soft }\varphi)}$ to third order in μ. The third-order term is

$$V^{(\mu^3)} = \mu^3 \int_p \frac{1}{\epsilon_p^2}. \tag{5.14}$$

In four dimensions, this is the logarithmically divergent integral

$$V^{(\mu^3)} = \frac{\mu^3}{8\pi^2}\int_0^\infty \frac{p^3 dp}{\epsilon_p^2} = \frac{m^2\mu^3}{4\pi^2}\int_0^\infty \frac{d\epsilon_p}{\epsilon_p}. \tag{5.15}$$

But, from the discussion surrounding Eq. (5.13), we know that this logarithm is cutoff in the infrared by the energy scale μ, due to the necessity of resummation, and in the ultraviolet by the energy scale ϕ_0, the energy scale where the self-energies are no longer well approximated by their zero-momentum values. Thus, even though we cannot easily compute the constant under the logarithm, we can write[11]

$$V^{(\mu^3)} = \frac{m^2\mu^3}{4\pi^2}\left[\ln\left(\frac{\phi_0}{\mu}\right) + O(1)\right]. \tag{5.16}$$

We can now use this to obtain the explicit logarithm shown in our final result (1.7) for ξ beyond NNLO by including Eq. (5.16) in the analysis of Sec. IV. Because $\partial V^{(\mu^3)}/\partial\phi_0$ does not have a logarithm, there is no logarithm in the NNNLO result for the location ϕ_0 of the minimum of the effective potential. The logarithm appears in ξ only through its effect on the density $n=-\partial V/\partial\mu$. Equation (4.8) for n is modified to

$$n = \frac{1}{\epsilon}\left(\frac{m\phi_0}{2\pi}\right)^{d/2}\left[1 + b_1\epsilon + b_2\epsilon^2 + \frac{\epsilon\mu}{\phi_0} - \frac{3\epsilon\mu^2}{\phi_0^2}\ln\frac{\phi_0}{\mu} + O(\epsilon^3)\right], \tag{5.17}$$

giving

$$\xi \equiv \frac{\mu}{\epsilon_F} = \frac{\epsilon^{2/d}\mu}{\phi_0}\left\{\tfrac{1}{2}\Gamma\left(\tfrac{d}{2}+1\right)\left[1 + b_1\epsilon + b_2\epsilon^2\frac{\epsilon\mu}{\phi_0} - \frac{3\epsilon\mu^2}{\phi_0^2}\ln\frac{\phi_0}{\mu} + O(\epsilon^3)\right]\right\}^{-2/d}. \tag{5.18}$$

Substituting the expectation (4.7) for ϕ_0 then produces the NNNLO logarithm shown in the final result (1.7) for ξ.

VI. EXTRAPOLATION OF ξ AT $d=3$

Because of the large relative size of the $O(\epsilon^{7/2})$ term in our result (1.7) for ξ, the next-to-next-to-leading-order (NNLO) result will likely only be useful in conjunction with more sophisticated analysis of dimension dependence than the naive prescription of setting $\epsilon=1$. In this respect, the situation appears somewhat analogous to the ϵ expansion for the critical exponent ω in the Ising model. ω is the exponent characterizing corrections to scaling, and its ϵ expansion is [12]

$$\omega_{\text{Ising}} = \epsilon - 0.629\,63\epsilon^2 + 1.618\,22\epsilon^3 + O(\epsilon^4). \tag{6.1}$$

Despite the large size of the NNLO ϵ^3 term, historical analysis using the terms shown above gave $\omega \simeq 0.79$ with a simple Borel-Padé approximation [9]. The latter is within a few percent of the correct result.[12]

Unfortunately, the ratio ξ does not have as simple an analytic structure as do critical exponents. Our result for ξ may be written as

$$\xi = \tfrac{1}{2}\epsilon^{1+2/d}b(\epsilon) \tag{6.2}$$

with

$$b(\epsilon) = 1 - 0.049\,16\epsilon - 0.959\,61\epsilon^2 - \tfrac{3}{8}\epsilon^3\ln\epsilon + O(\epsilon^{9/2}). \tag{6.3}$$

Critical exponents have a simple asymptotic expansion in powers of ϵ. But, even if we factor out the overall $\epsilon^{1+2/d}$ and focus only on $b(\epsilon)$ above, our expansion contains powers of $\ln\epsilon$.

The Borel transform of a series

$$f(\epsilon) = \sum_n f_n\epsilon^n \tag{6.4}$$

is the faster-converging series

$$F(t) = \sum_n \frac{f_n}{n!}t^n. \tag{6.5}$$

The original $f(\epsilon)$ may be recovered from its Borel transform by

$$f(\epsilon) = \int_0^\infty dt e^{-t}F(\epsilon t) \tag{6.6}$$

if $F(t)$ does not have any singularities on the positive real axis which make the integral ill defined. The standard approach for critical exponents is to fit some type of Padé-like approximation to the Borel transform. A simple $[M/N]$ Padé approximation would be

$$F(t) = \frac{1 + p_1 t + p_2 t^2 + \cdots p_M t^M}{1 + q_1 t + q_2 t^2 + \cdots q_N t^N}, \tag{6.7}$$

[11] The coefficient of this logarithm has also been computed by Nishida [17].

[12] See, for instance, the results for $\theta=\omega\nu$ and ν from three-dimensional (3D) series techniques, the ϵ expansion, numerical Monte Carlo simulations, and experiments all reviewed in Ref. [12] for the $O(N)$ model. (The Ising universality class corresponds to $N=1$ in these tables.) The current results presented there for ω from 3D series techniques and the ϵ expansion are 0.799(11) and 0.814(18).

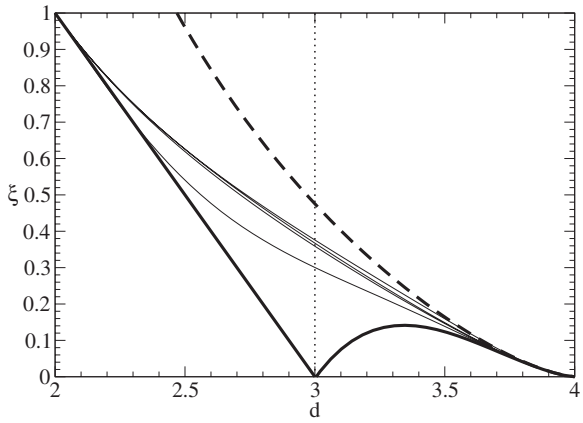

FIG. 13. Extrapolations of ξ vs dimension d. The thin solid lines show the result of Padé-Borel extrapolations of type [4/0], [2/2], [3/1], and [0/4] from bottom to top. For comparison, the thick solid lines show simple truncations of the expansions about four (right) and two (left) dimensions, as discussed in the text. The thick dashed line is the truncated $d=4-\epsilon$ expansion at NLO rather than NNLO.

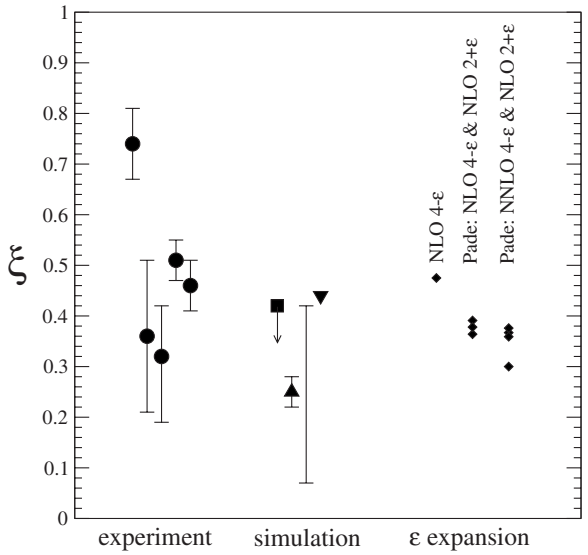

FIG. 14. A selection of estimates of ξ in three spatial dimensions. Experimental values (circles) include 0.74(7) [18], 0.34(15) [19], $0.32^{+0.13}_{-0.10}$ [20], and the more recent 0.51(4) [8] and 0.46(5) [21]. Simulations include fixed-node Green's function and diffusion Monte Carlo upper bounds of 0.42(1) [4] (square). Other simulation methods have estimated 0.22(3) [22], $0.07 \leq \xi \leq 0.42$ [23], and ≈ 0.44 [24] (the last two are based on finite-temperature calculations). The NLO $4-\epsilon$ value is that of Eq. (1.6) [6]. The rest are the Padé-Borel estimates discussed in this section, with the purely NLO result from Ref. [13].

where we assume $f(\epsilon)$ is normalized so that $f(0)=1$. More sophisticated versions have been used for accurate estimates to critical exponents from high-order ϵ expansions. However, such estimates must necessarily break down for the Borel transform $B(t)$ of Eq. (6.3) because of the $\ln \epsilon$ terms. The appearance of $\ln \epsilon$ in the small ϵ expansion of $b(\epsilon)$ gives rise to $\ln t$ terms in the small t expansion of its Borel transform, and these are not accommodated by Padé approximants such as Eq. (6.7).[13]

Clearly, what is needed to make full use of ϵ expansion results is a full understanding of the analytic structure of $\xi(\epsilon)$ in ϵ, in order to inform the strategy for how best to extrapolate to $d=3$. Nonetheless, it is interesting to see what happens if one naively extrapolates $\xi(\epsilon)$ using simple Padé estimates (6.7) to the Borel transform $B(t)$. This was carried out by Nishida and Son in Ref. [13], constraining the Padé approximants by (i) the next-to-leading-order (NLO) result near the expansion of ξ in $4-d$, and (ii) a next-to-leading-order result for the expansion of ξ in $d-2$. Since the leading-order $4-d$ result has already been used to normalize $b(0)=1$ above, this represents three constraints on $B(t)$, and so the possible Padé approximants are those with $M+N=3$. Extrapolating to three dimensions, they then found $\xi=0.391$, 0.364, and 0.378 with [3/0],[1/2], and [0/3] Padé approximants. They did not find any solution satisfying the constraints for a [2/1] approximant. These values for ξ span 0.378 ± 0.014.

If we naively follow the same procedure but add the information from our NNLO coefficient, we find $\xi=0.300$, 0.367, 0.359, and 0.376 in three dimensions from [4/0], [3/1], [2/2], and [0/4] approximants. We did not find a solution for [1/3]. The [4/0] value is an outlier, which makes a certain amount of sense. [4/0] corresponds to a simple polynomial form for $B(t)$. This does not allow for any singularities in the Borel plane and so will not produce an asymptotic series in ϵ, whereas the large NNLO coefficient suggests that the asymptotic nature of the expansion should not be ignored at this order. If we focus only on the other values, they span $\xi=0.367 \pm 0.009$. This is consistent with the NLO results, but not an obvious improvement. The fits of ξ as a function of d are shown in Fig. 13 and are quite similar to the earlier fits of Ref. [13] discussed above which did not use the NNLO result for $d=4-\epsilon$.

For comparison, the same figure also shows the result of avoiding any fancy extrapolation but simply naively using the truncated NNLO result $\xi=\frac{1}{2}\epsilon^{1+2/d}[1-0.049\,16\epsilon-0.959\,61\epsilon^2]$ for $d=4-\epsilon$ or the corresponding NLO result $\xi=1-\bar{\epsilon}$ of Ref. [13] for $d=2+\bar{\epsilon}$. It is amusing that both of these naive extrapolations happen to give consistent values of $\xi \simeq 0$ at $d=3$. We imagine that this is a coincidence.

Figure 14 summarizes a selection of estimates of ξ from experiment and numerical simulations, and compares them to results obtained so far from the ϵ expansion. The current Padé-Borel extrapolated ϵ expansion results, however, need to be taken with a significant grain of salt because their assumptions of analytic structure are not consistent with what we have learned in Sec. V about higher-order corrections. Further study will be required to develop more consistent extrapolations.

[13]Specifically, the Borel transform of $b(\epsilon)=1+\alpha\epsilon+\beta\epsilon^2+\gamma\epsilon^3 \ln \epsilon + \delta\epsilon^3$ is $B(t)=1+\alpha t+\frac{1}{2!}\beta t^2+\frac{1}{3!}\gamma t^3 \ln t+\frac{1}{3!}[\delta-\gamma\psi(4)]t^3$, where $\psi(z)$ is the digamma function. This can be demonstrated by checking Eq. (6.6).

ACKNOWLEDGMENTS

We would like to thank Yusuke Nishida for useful conversations. One of us (P.A.) would like to thank Eric Braaten for encouragement to become involved in this problem. This work was supported, in part, by the U.S. Department of Energy under Grant No. DE-FG02-97ER41027 and Grant No. DE-FG02-00ER41132.

APPENDIX A: SUMMARY OF RESULTS BY DIAGRAM TYPE

Figure 4(a):

$$V_1^{(0)} = -\int_p E_p = \phi_0\left(\frac{m\phi_0}{2\pi}\right)^{d/2}\frac{\Gamma\left(-\frac{1}{2}-\frac{d}{4}\right)}{2^{1+\frac{d}{2}}\Gamma\left(\frac{1}{2}+\frac{d}{4}\right)}$$

$$= \phi_0\left(\frac{m\phi_0}{2\pi}\right)^{d/2}\frac{1}{3}\left\{1+\frac{1}{2}\left(\tfrac{7}{3}-\gamma-\ln 2\right)\epsilon + \left[\tfrac{1}{8}\left(\tfrac{7}{3}-\gamma-\ln 2\right)^2+\tfrac{19}{72}\right]\epsilon^2+O(\epsilon^3)\right\}.$$

Figure 4(b):

$$V_1^{(\mu)} = +\mu\int_p \frac{\epsilon_p}{E_p} = \mu\left(\frac{m\phi_0}{2\pi}\right)^{d/2}\frac{\Gamma\left(-\frac{d}{4}\right)}{2^{d/2}\Gamma\left(\frac{d}{4}\right)}$$

$$= -\frac{\mu}{\epsilon}\left(\frac{m\phi_0}{2\pi}\right)^{d/2}\left\{1+\tfrac{1}{2}\left(\tfrac{1}{2}-\gamma+\ln 2\right)\epsilon + \left[\tfrac{1}{8}\left(\tfrac{1}{2}-\gamma+\ln 2\right)^2+\tfrac{1}{32}\right]\epsilon^2+O(\epsilon^3)\right\}.$$

Figure 4(c):

$$V_1^{(\mu\mu)} = -\tfrac{1}{2}\mu^2\phi_0^2\int_p \frac{1}{E_p^3} = -\frac{\mu^2}{\phi_0}\left(\frac{m\phi_0}{2\pi}\right)^{d/2}\frac{\Gamma\left(\frac{3}{2}-\frac{d}{4}\right)}{2^{\frac{d}{2}}\Gamma\left(\frac{1}{2}+\frac{d}{4}\right)} =$$

$$-\frac{\mu^2}{\phi_0}\left(\frac{m\phi_0}{2\pi}\right)^{d/2}\frac{1}{2}\{1+O(\epsilon)\}.$$

Figure 5(a): See Eqs. (3.19) through (3.23).
Figures 5(a)–5(d):

$$V_2^{(\mu)} = -\mu g^2\phi_0^2\int_{pq}\frac{(E_p-\epsilon_p)}{2E_pE_q^2\mathcal{S}_{pq}}\left(\frac{1}{E_q}+\frac{1}{S_{pq}}\right) = \mu\left(\frac{m\phi_0}{2\pi}\right)^{d/2}[\epsilon K_2^{(\mu)}+O(\epsilon^2)], \tag{A4}$$

$$K_2^{(\mu)} \simeq -0.25835. \tag{A5}$$

Figure 6(a): See Eqs. (3.8), (3.14), and (3.17).
Figures 6(b)–6(d):

$$V_3^{(\Sigma\Sigma)} = g^4\int_{pqk}\frac{(E_p-\epsilon_p)(E_q-\epsilon_q)}{2E_p2E_q(2E_k)^2}\left[\frac{2(E_k-\epsilon_k)^2}{\mathcal{S}_{pk}^2\mathcal{S}_{qk}} - \phi_0^2\left(\frac{2}{E_k\mathcal{S}_{pk}\mathcal{T}_{pq,k}}+\frac{2}{\mathcal{S}_{pk}^2\mathcal{T}_{pq,k}}+\frac{1}{E_k\mathcal{S}_{pk}\mathcal{S}_{qk}}\right)\right] = \phi_0\left(\frac{m\phi_0}{2\pi}\right)^{d/2}[\epsilon^2K_3^{(\Sigma\Sigma)}+O(\epsilon^3)], \tag{A6}$$

$$K_3^{(\Sigma\Sigma)} \simeq -0.03046. \tag{A7}$$

Figure 6(e):

$$V_3^{(\widetilde{\Pi\Pi})} = -g^4\phi_0^4\int_{pqk}\frac{1}{2E_p2E_q2E_k2E_l\mathcal{S}_{pk}\mathcal{S}_{ql}}\left[\frac{1}{\frac{1}{2}\epsilon_{p+k}}+\frac{1}{\mathcal{E}_{pqkl}}\right] = \phi_0\left(\frac{m\phi_0}{2\pi}\right)^{d/2}[\epsilon^2K_3^{(\widetilde{\Pi\Pi})}+O(\epsilon^3)], \tag{A8}$$

$$K_3^{(\widetilde{\Pi\Pi})} \simeq -0.31080. \tag{A9}$$

Figures 6(f)–6(h): See Eqs. (3.44), (3.39), and (3.43)

We have used the shorthand notation of Eq. (3.9). In the momentum integrals shown in Eqs. (A4) and (A6), we have used symmetry to simplify the expressions. For expressions that correspond to simply doing the frequency integrals of these diagrams without using such symmetry, simply symmetrize the integrands under $\boldsymbol{p}\leftrightarrow\boldsymbol{q}$.

APPENDIX B: WHAT HAPPENED TO $\theta(\mu-\epsilon_p)$?

In this appendix, we give a quick, illustrative example of the effect of ϕ_0 on what otherwise would be a Fermi-sea step-function $\theta(\mu-\epsilon_p)$. The example will be the mean-field theory result for the fermion number density n in the presence of both a non-negligible chemical potential μ and a condensate ϕ_0. In terms of diagrams, this corresponds to the one-loop fermion diagram of Fig. 4(b) if we take the cross to represent the fermionic number operator and (unlike the rest of this paper) include the chemical potential μ in the fermion propagator rather than treating it as a perturbation. It will be clearer if we give a regularization-independent version of the result rather than continuing to work in dimensional regularization. In terms of diagram evaluation, this can be achieved by subtracting the vacuum contribution ($\mu=\phi=0$) to n before doing any integrals. The result, after frequency integration, is then the standard mean-field formula for the number equation[14]

$$n = \int_p\left(1-\frac{\epsilon_p^\mu}{E_p^\mu}\right) = \int_p\left(1-\frac{(\epsilon_p-\mu)}{[(\epsilon_p-\mu)^2+\phi_0^2]^{1/2}}\right). \tag{B1}$$

In the limit $\phi_0\to 0$, the above formula gives the usual result for a free fermion gas:

[14]For comparison, the result to leading order in μ in dimensional regularization could be obtained by applying $n=-\partial V/\partial\mu$ to the result $V_1=-\int_p E_p^\mu$ discussed in Sec. III E, giving $n=-\int_p\epsilon_p^\mu/E_p^\mu$ in dimensional regularization. This appears to differ from Eq. (B1) by $\int_p 1$, but $\int_p 1$ vanishes in dimensional regularization.

$$n = 2\int_p \theta(\mu - \epsilon_p).$$

It would be problematical to treat μ perturbatively in such an expression. However, in the opposite limit $\mu \ll \phi_0$ relevant to this paper, there is no obstruction to treating μ perturbatively. To leading order in μ,

$$n = \int_p \left(1 - \frac{\epsilon_p}{E_p}\right).$$

We thus find fractions involving energies rather than θ functions, similar to results we have derived for other diagrams in this paper.

[1] D. R. Eagles, Phys. Rev. **186**, 456 (1969); A. J. Leggett, in *Modern Trends in the Theory of Condensed Matter*, edited by A. Pekalski and J. Przystawa (Springer-Verlag, Berlin, 1980); P. Nozières and S. Schmitt-Rink, J. Low Temp. Phys. **59**, 195 (1985); M. Randeria, in *Bose-Einstein Condensation*, edited by A. Griffin *et al.* (Cambridge University Press, Cambridge, England, 1995).

[2] T. L. Ho, Phys. Rev. Lett. **92**, 090402 (2004).

[3] G. A. Baker Jr., Int. J. Mod. Phys. B **15**, 1314 (2001); H. Heiselberg, Phys. Rev. A **63**, 043606 (2001).

[4] J. Carlson, S.-Y. Chang, V. R. Pandharipande, and K. E. Schmidt, Phys. Rev. Lett. **91**, 050401 (2003); G. E. Astrakharchik, J. Boronat, J. Casulleras, and S. Giorgini, *ibid.* **93**, 200404 (2004); J. Carlson and S. Reddy, *ibid.* **95**, 060401 (2005).

[5] Z. Nussinov and S. Nussinov, Phys. Rev. A **74**, 053622 (2006); Z. Nussinov and S. Nussinov, e-print cond-mat/0410597.

[6] Y. Nishida and D. T. Son, Phys. Rev. Lett. **97**, 050403 (2006).

[7] C. Menotti, P. Pedri, and S. Stringari, Phys. Rev. Lett. **89**, 250402 (2002).

[8] J. Kinast, A. Turlapov, J. E. Thomas, Q. Chen, J. Stajic, and K. Levin, Science **307**, 1296 (2005).

[9] E. Brézin, J. C. Le Guillou, and J. Zinn-Justin, Phys. Rev. D **15**, 1544 (1977).

[10] J. C. Le Guillou and J. Zinn-Justin, J. Phys. (Paris), Lett. **46**, L137 (1885); J. Phys. (Paris) **48**, 19 (1987); **50**, 1365 (1989);

[11] C. Bervillier, Phys. Rev. B **34**, 8141 (1986).

[12] R. Guida and J. Zinn-Justin, J. Phys. A **31**, 8103 (1998).

[13] Y. Nishida and D. T. Son, e-print cond-mat/0607835.

[14] J. Zinn-Justin, *Quantum Field Theory and Critical Phenomena*, 3rd ed. (Clarendon Press, Oxford, 1996).

[15] M. E. Peskin and D. V. Schroeder, *An Introduction to Quantum Field Theory* (Addison-Wesley, Reading, MA, 1995).

[16] G. Baym, J.-P. Blaizot, and J. Zinn-Justin, Europhys. Lett. **49**, 150 (2000); P. Arnold, G. D. Moore, and B. Tomasik, Phys. Rev. A **65**, 013606 (2002).

[17] Y. Nishida (private communication).

[18] K. M. O'Hara, S. L. Hemmer, M. E. Gehm, S. R. Granade, and J. E. Thomas, Science **298**, 2179 (2002); M. E. Gehm, S. L. Hemmer, S. R. Granade, K. M. O'Hara, and J. E. Thomas, Phys. Rev. A **68**, 011401(R) (2003).

[19] T. Bourdel, L. Khaykovich, J. Cubizolles, J. Zhang, F. Chevy, M. Teichmann, L. Tarruell, S. J. J. M. F. Kokkelmans, and C. Salomon, Phys. Rev. Lett. **93**, 050401 (2004).

[20] M. Bartenstein, A. Altmeyer, S. Riedl, S. Jochim, C. Chin, J. H. Denschlag, and R. Grimm, Phys. Rev. Lett. **92**, 120401 (2004).

[21] G. B. Partridge, W. Li, R. I. Kamar, Y. Liao, and R. G. Hulet, Science **311**, 503 (2006).

[22] D. Lee, Phys. Rev. B **73**, 115112 (2006).

[23] D. Lee and T. Schäfer, Phys. Rev. C **73**, 015202 (2006).

[24] A. Bulgac, J. E. Drut, and P. Magierski, Phys. Rev. Lett. **96**, 090404 (2006).